

Article

Morphological Features and Spectral Comparisons of Diamonds from Three Kimberlite Belts in Mengyin, China

Chao-Fan Zhang^{1,2}, Fei Liu^{1,3,4,*}, Qing Lv⁴, Yun Wang⁵ and Jing-Sui Yang^{1,3,4,5}

¹ Key Laboratory of Deep-Earth Dynamics, Institute of Geology, Chinese Academy of Geological Sciences, Beijing 100037, China

² Institute of Geophysics and Geomatics, China University of Geosciences, Wuhan 430074, China

³ Southern Marine Science and Engineering Guangdong Laboratory (Guangzhou), Guangzhou 511458, China

⁴ Shandong Academician Workstation of Diamond Mineralization Mechanism and Exploration, Shandong No. 7 Exploration Institute of Geology and Mineral Resources, Linyi 276006, China

⁵ School of Earth Sciences and Engineering, Nanjing University, Nanjing 210023, China

* Correspondence: liufei@cags.ac.cn or lfhy112@126.com

Abstract: Striking differences in potentiality of diamond mineralization are shown in the three kimberlite belts of Changmazhuang, Xiyu and Poli in Mengyin, Shandong Province. Previous studies of diamonds have focused on the Changmazhuang belt; however, genesis of diamonds from the other two belts, as well as comparative studies on diamonds from the three belts, are relatively scarce. In this paper, the morphological and spectral features of 44 diamonds ranging from 0.03 mg to 16.46 mg in weight from the three belts are investigated systematically by microscopic observation, Fourier-transform infrared spectroscopy (FTIR) and Raman spectroscopy. The results show that the formation temperature is 1118–1251 °C for Changmazhuang diamonds, 1091–1167 °C for Xiyu diamonds, and 1132–1172 °C for Poli diamonds. Diamonds in the three belts exhibit uniform pre-kimberlite surface features of multiple serrate, triangular laminae and small trigons, suggesting a similar condition of diamond destructive metasomatism caused by carbonatitic and silicate-carbonatitic melts. However, Poli diamonds probably suffered from a silicate component-enriched carbonatitic melt in the deep mantle. Nitrogen contents (0–539 ppm) of diamonds from the three belts have a slight impact on their morphological features.

Keywords: Mengyin; kimberlitic diamond; morphological features; FTIR; Raman spectroscopy



Citation: Zhang, C.-F.; Liu, F.; Lv, Q.; Wang, Y.; Yang, J.-S. Morphological Features and Spectral Comparisons of Diamonds from Three Kimberlite Belts in Mengyin, China. *Minerals* **2022**, *12*, 1185. <https://doi.org/10.3390/min12101185>

Received: 1 August 2022

Accepted: 15 September 2022

Published: 21 September 2022

Publisher's Note: MDPI stays neutral with regard to jurisdictional claims in published maps and institutional affiliations.



Copyright: © 2022 by the authors. Licensee MDPI, Basel, Switzerland. This article is an open access article distributed under the terms and conditions of the Creative Commons Attribution (CC BY) license (<https://creativecommons.org/licenses/by/4.0/>).

1. Introduction

Natural diamonds are a unique probe into the geochemical composition, redox state and geodynamic process of the interior earth from the subcontinental lithospheric mantle root between 120 and 250 km in depth, through the transition zone ranging from 410 to 660 km, and at far greater depths of 700–800 km [1,2]. The resorption (dissolution) of diamonds due to mantle metasomatism mainly occurs during residence in the mantle (pre-kimberlite) and later ascent to the surface via mantle convection by alkaline magmas, e.g., kimberlite, lamproite [2–4]. Therefore, the surface textures and morphology could provide a robust tool for investigating the growth conditions and dissolution environment of diamonds [5,6]. Diamonds record an extreme variety of kinds of resorption characteristics on their surface. It has been confirmed that the rounding of the edges of octahedra and cubic diamonds and their transformation into tetra-hexahedron (THH) occurs due to interactions with the host kimberlite magma [7,8]. Except surface textures due to kimberlite magma's upward migration, some diamonds enclosed inside mantle xenoliths during the whole duration of ascent in kimberlite magma can preserve surface features inherited from the mantle (pre-kimberlite surface features). Some resorption features can be identified well by various spectral and optical patterns of diamond [9,10]. A study of numerous diamond crystals from eclogitic xenoliths showed that diamonds recovered from inside xenoliths

preserve an octahedral shape with sharp edges, but show dissolution features on {111} faces [11]. These pre-kimberlitic dissolution events record the last diamond-destructive metasomatic event to have occurred in the mantle, of great significance for exploring the mantle environment.

The diamondiferous kimberlite cluster in Mengyin, Shandong Province, including Changmazhuang, Xiyu and Poli kimberlitic belts, is an important production area of diamonds in China. There are significant differences in kimberlitic mineralization, lithological assemblage, various degrees of carbonation, crystal color, grain size, morphological and surface features and inclusion of diamonds in the three belts [12,13]. The Shengli I kimberlite pipe in Changmazhuang belt, as the richest diamond mine in the Mengyin deposit, produces high-grade diamond and high-value brown diamond [12]. In contrast, the Poli diamondiferous kimberlite belt has not found industrial value diamond. It is ambiguous whether the formation stages and depth, temperature and pressure condition of diamonds in the three belts are different. In this paper, we present the optical and spectral features of 44 diamond grains from the three belts using high-definition microscope, FTIR spectroscopy and Raman spectroscopy. Types of diamond by FTIR spectra and nitrogen contents of diamond by software QUIDDIT (quantification of infrared active defects in diamond and inferred temperatures) are investigated [14]. The temperature and pressure are calculated by the conversion rate from center A to center B of nitrogen in diamonds and their inclusions. Their surface features and spectral data show that diamonds formed in the multi-stages involved in the pre-kimberlite stage of mantle residence and the upward migration stage of being brought to the surface of the earth by kimberlitic magma. These new values and interpretation provide new insights into the origin and genesis of Mengyin diamond in the three kimberlite belts.

2. Geological Setting

Natural diamond deposits with economic value in China basically occur in (1) Mengyin, Shandong province (Figure 1a), (2) Wafangdian (also named Fuxian in the past), Liaoning province, and (3) Hunan province along the Yuanshui River Basin. The former two deposits host kimberlite are derived from alluvial sediments and crop out within the Hebei–Shandong–Liaoning continental core in the eastern part of the North China Craton. The Mengyin diamonds are produced from Early Paleozoic kimberlite and various ages of alluvial rocks, the former located in the area about 60–70 km west of Tancheng-Lujiao fault (Figure 1b). The diamondiferous kimberlite deposit consists of Changmazhuang, Xiyu and Poli kimberlite belts from south west to north east (Figure 1c). The overall striking of the Mengyin deposit is about NNE 55°, with a length of about 55 km and a width of 15 km in total. There are 10 pipes, 47 dikes and one sill in the three belts. The wall-rocks are briefly composed of Neoproterozoic Trondhjemite, Tonalite, Granodiorite (TTG) gneiss and Neoproterozoic Taishan Group strata, Paleoproterozoic intrusive rocks and minor Cambrian limestone [13]. In a panoramic view, they are characterized by a trend of spreading to the north and converging to the south. If the center points of the three rock belts are connected in turn, the connecting line is a broken line protruding from the northwest, and the distance between the center points is about 22 km, so its directivity, equidistance and left-column distribution are obvious.

The Changmazhuang belt is located in the west of Changma village, about 13 km southwest of Mengyin County, with a total strike of NW 345°, a length of about 14 km and a width of 2.5 km (Figure 1c). It consists of eight kimberlite dikes and two pipes, eight of which are of industrial grade, and all the dikes are arranged in the right column, among which Shengli I contains the highest grade of pipes, reaching 600–800 mg/m³ (the lowest industrial grade is 15 mg/m³) [15]. The lithology of Changmazhuang rock belt is mainly porphyritic kimberlite, with a high content of pyrope.

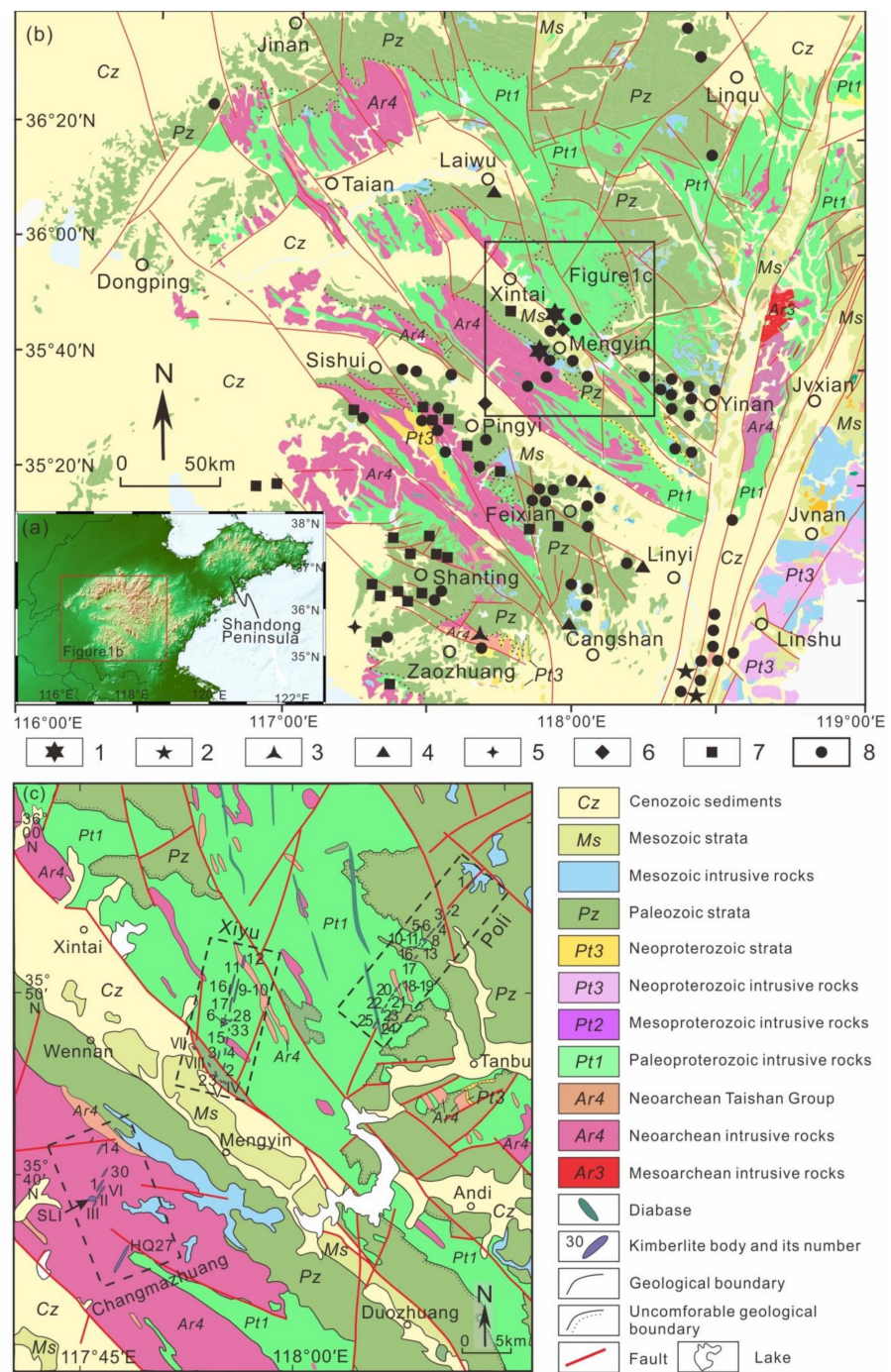


Figure 1. (a) Simplified topographic map of Shandong Peninsula. (b) Distribution map of kimberlite-hosted diamonds and alluvial rocks-derived diamonds in Shandong Province. 1-kimberlite-hosted diamond; 2-Alluvial diamond; 3-Diamond-bearing conglomerate in Cambrian Liguan Formation; 4-Diamond-bearing conglomerate in Carboniferous Benxi Formation; 5-Diamond-bearing conglomerate in Jurassic Sanhe Formation; 6-Diamond-bearing conglomerate in Paleogene Gucheng Formation; 7-Diamond-bearing conglomerate in Neogene-Quaternary Baiyan Formation; 8-Diamond-bearing Quaternary conglomerate [16]; (c) Geological map of diamonds hosted in the Changmazhuang, Xiyu and Poli kimberlite belts in Mengyin deposit. Greek numbers I, II, III and VI in the Changmazhuang belt and IV, V, VII and VIII in the Xiyu belt should be preceded by Shengli (means victory, SL in short) as SL I–VIII; Roman numbers 1–30 in the two belts should be preceded by Hongqi (means red flag, HQ in short) as HQ1–30; Roman numbers 1–25 in the Poli belt should be preceded by K as K1–25 to number kimberlite bodies.

The Xiyu belt is located near Xiyu village, about 12 km north of Mengyin County, with a total strike of about 15° , a length of about 12 km and a width of 0.5–1 km. It is composed of 24 kimberlite bodies, of which 17 are of industrial grade and they can be divided into NNE-trending rock belt and NW-trending rock belt according to the distribution direction of the dikes. The industrial grade ranges from 204.16 mg/m^3 to 24.96 mg/m^3 . The main lithology of the dikes is phlogopite-bearing porphyritic kimberlite. The rock mainly consists of porphyritic phlogopite kimberlite, kimberlite breccia, porphyritic magnesite kimberlite and fine-grained kimberlite [15].

The Poli belt is located in Yedian–Poli–Jinxingtou area of Daigu town, 30 km northeast of Mengyin County with a total strike of about NE $35\text{--}45^\circ$, a length of about 18 km and a width of about 0.6 km. It consists of 25 dikes, no pipes, poor ore-bearing properties and no bodies reaching industrial grade. The dike strike is basically consistent with the Poli belt. Most are in an intermittent or echelon arrangement, and the main lithology is porphyritic phlogopite kimberlite [17]. In all, the diamond-bearing kimberlitic rocks in the three belts follows a rule that diamonds are enriched in the south and poor in the north [18].

All previous studies of surface resorption of Shandong diamond are aimed at the comparison of the surface texture, and diamond samples mainly from Shengli I pipe in the Changmazhuang belt [12,15], while there is little research on the diamond resorption in the other two belts of Xiyu and Poli [18]. Therefore, it is unclear whether the surface characteristics of diamonds in the three kimberlite belts are consistent. The research on the diamond resorption of three kimberlites in Shandong is limited to the types of diamond resorption, hardly discussing the origins of their formation [18].

3. Materials and Methods

3.1. Materials

In this study, 44 samples from Changmazhuang, Xiyu and Poli belts are investigated with the weight ranging from 0.03 mg to 16.46 mg. Of these, 8 diamonds are from Shengli I (SLI) and 6 diamonds are from Hongqi 27 (HQ27) in the Changmazhuang belt; 15 diamonds from Hongqi 23 (HQ23) in Xiyu belt; and 15 diamonds are from the Poli belts. Each sample was cleaned with 75% alcohol to remove dust and grease on the surface.

3.2. Methods

Three-dimensional pictures and microscopic examination were performed by a high-definition Leica M205C microscope in the School of Earth Sciences and Engineering, Nanjing University. This allowed clear investigation of the surface features and texture of the studied diamonds.

All samples were analyzed by FTIR spectroscopy at the Institute of Geology, Chinese Academy of Geological Sciences. The FTIR instrument is a HYPERION2000 microscope with a liquid nitrogen-cooled Bruker Vertex 70V spectrometer. The spectra were obtained by software OPUS, FTIR absorption spectra range from 4000 cm^{-1} to 600 cm^{-1} was collected with a resolution of 2 cm^{-1} and background spectra of 32 scans were recorded before the analytical session.

The nitrogen contents and different aggregation states of the studied diamonds were calculated by QUIDDIT, which is a free Python software-package designed to process FTIR spectra of diamonds automatically and efficiently. Its core capabilities include baseline correction, determination of nitrogen concentration, nitrogen aggregation state and model temperature and fitting of both the 3107 cm^{-1} and platelet peaks. QUIDDIT has been used successfully for natural diamonds containing aggregated forms of nitrogen as well as diamonds containing C-centers [14].

Raman spectra were acquired by a Renishaw InVia Reflex Raman confocal microspectrometer with $15\times$ objective lens at Shandong No. 7 Exploration Institute of Geology and Mineral Resources. The excitation light source was a solid laser with wavelength of 532 nm and 50 mW. The test environment was at room temperature (21°C , humidity 30%), laser power with energy of 5%, 50 times objective lens, zero focus, scanning time of

1 s, scanning 3 times, and scanning range of 200–2000 cm^{-1} with a resolution of 1 cm^{-1} . The diamond sample to be tested was washed with absolute ethyl alcohol. In addition, according to the condition of the sample surface, the power of the Raman instrument was modified to obtain accurate and effective data. The Raman spectra of diamond inclusions were obtained by adjusting the laser power, exposure time and accumulations via WiRE 5.2 software (Renishaw Trading Company Ltd., Gloucestershire, UK).

4. Results

4.1. Microscopic Examination

The microscopic observation of 44 diamond grains was acquired by an optical microscope and the surface features and inclusions within diamonds are shown as follows:

- (1) Studied diamonds have commonly suffered from strong corrosion and growth stress; however, the degrees of damage, resorption and crystal integrity of diamonds in the three belts are different.
- (2) Samples from the Poli belt are the most damaged and the crystal shape of diamond is the most incomplete. Octahedron corners are all rounded and the distribution of resorption texture on the surface is messy, along with most types of corrosion image.
- (3) Plastic deformation slip lines on the surface of diamonds from the Poli belt probably indicates that the Poli diamonds are subjected to strong stress.

Our investigated samples, as well as previous studies, suggest that the surface textures of diamonds in the three belts have different characteristics, mainly suggesting that the proportion of surface texture species, degree of surface corrosion and crystal damage are clearly different (Table 1). The surface texture types of diamonds in Changmazhuang and Xiyu belts are basically analogous, but the development ratios of different surface texture in these two belts are different. The main textures surface of diamonds in the Changmazhuang belt are triangular growth plates, triangular pits, tetragonal etch pits, terraces, drop-shaped hillocks, deformation lines and ruts (Figure 2a–f). The surface texture of growth hillock, triangular pits and growth steps shows a higher proportion in Xiyu belt (Figure 2g–i) [18]. The morphology of diamond in Poli belt is dominated by octahedron and fragments, so the surface texture mainly develops triangular pits, growth steps, growth hills, etc. (Figure 2j–l). Besides, the crystal morphology of diamond in Changmazhuang belt is relatively complete, followed by that in Xiyu, and the diamonds in Poli suffered the most serious resorption.

Table 1. Main surface features of diamonds from the three kimberlite belts in Mengyin, China.

Belt	Main Texture	Octahedral	Dodecahedral	Left
Changmazhuang	Triangular growth plates, triangular pits, tetragonal etch pits, terraces, Drop-shaped hillocks, Deformation lines, Ruts	9	0	6
Xiyu	Triangular growth plates, triangular pits, tetragonal etch pits, terraces, Drop-shaped hillocks, Deformation lines, Ruts	10	2	4
Poli	Triangular growth plates, triangular pits,	8	1	4

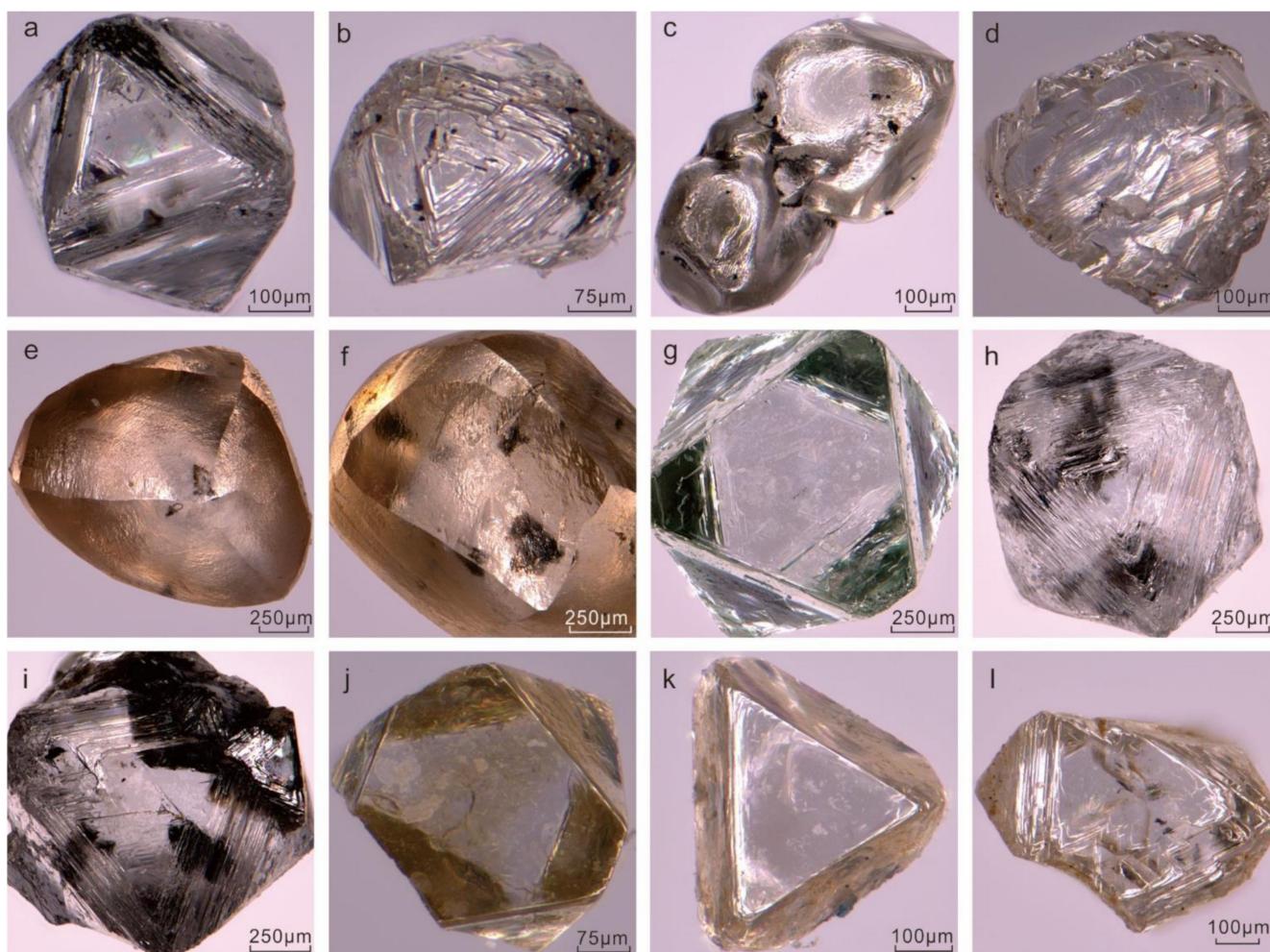


Figure 2. Microscopic 3-D pictures of diamonds in the three belts showing internal texture, surface features and inclusions. (a) Changmazhuang (SL-1) diamond, triangular plates; (b) Changmazhuang (SL-2), peak cluster triangular hill; (c) Changmazhuang (SL-3) terraces; (d) Changmazhuang (SL-7), deformation lines; (e) Changmazhuang (HQ27-2), Drop-shaped hillocks; (f) Changmazhuang (HQ27-3), imbricated etched figures; (g) Xiyu (HQ23-2), flat-bottomed trigons; (h) Xiyu (HQ23-13), triangular plates; (i) Xiyu (HQ23-15), peak cluster triangular hill; (j) Poli (35T10-2), octahedral fragment; (k) Poli (Q29-1), triangular plates; (l) Poli (QPL-2), few flat-bottomed trigons.

4.2. FTIR Spectra Features

The type of each studied diamond can be identified by typical characteristic peaks of the FTIR spectrum in reflection mode. In Figure 3, the infrared spectra of different samples in the range $1800\text{--}2700\text{ cm}^{-1}$ fully show the intrinsic peak of diamond, and the FTIR mapping of SL-2 has an obvious absorption peak at the C center (1282 cm^{-1}) (Figure 3e), which means it only has N pairs. HQ23-2 exhibits a typical IaAB pattern and contains H atoms (VN3H, FTIR at 3107 cm^{-1}) (Figure 3f), and H is the impurity with the most content in diamond except N.

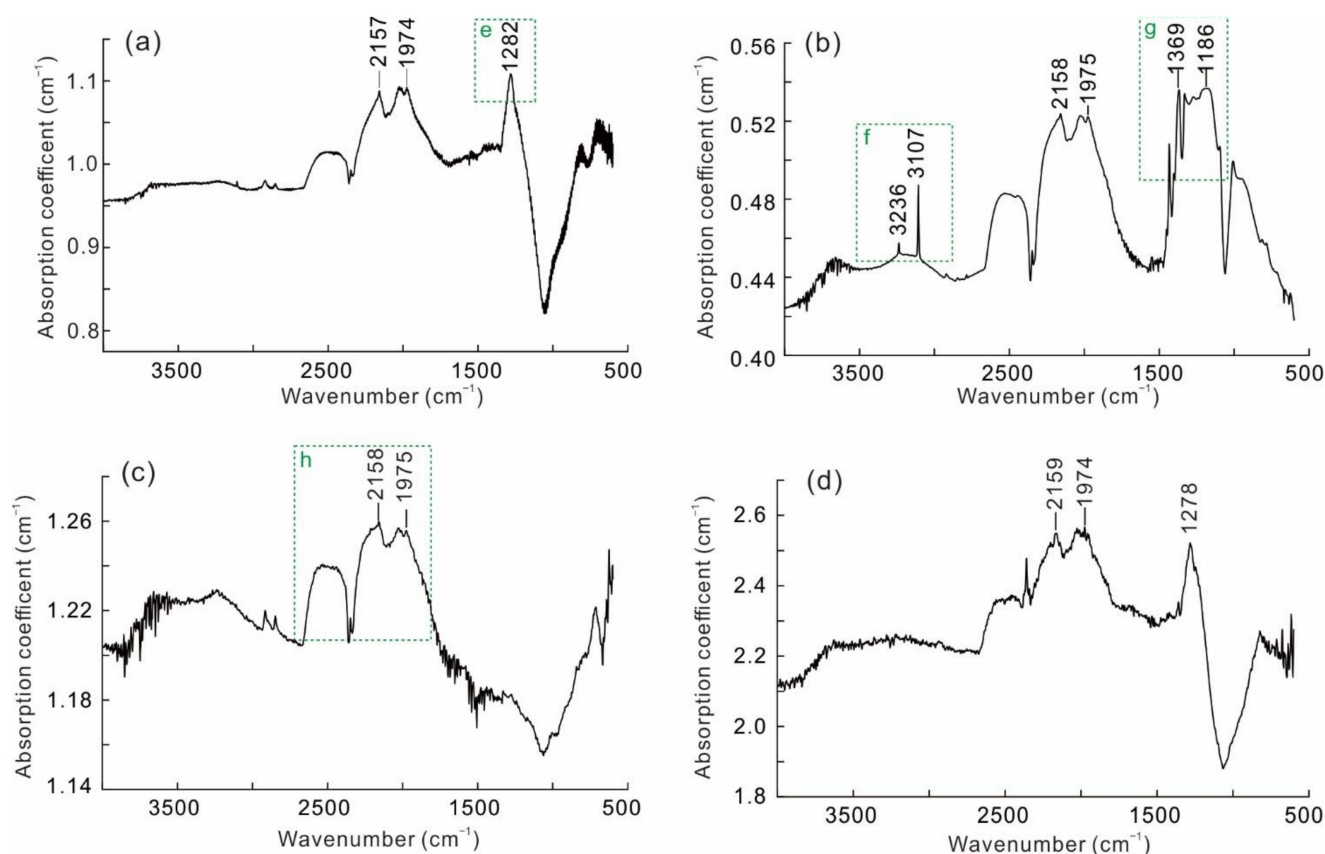


Figure 3. The FTIR strata of representative diamonds in three belts. (a): SL-2 (IaA), (b): HQ23-2 (IaAB), (c): Q29-1 (IIa), (d): PO-1 (IaA). e: C center; f: absorption features of H atoms, g: two-phonon region with intrinsic diamond absorption features; h: the typical feature of type IaAB diamond.

The majority types among the 44 studied diamonds in the three belts are IaAB and IaA and the diamonds from different belts show various main types. The types of SLI diamonds in Changmazhuang belt are mainly IaA (Figure 3a) with minor type II, while the HQ23 samples in the Xiyu belt are mainly IaAB (Figure 3b) and both types are observed in the Poli belt.

The content and aggregation state of N in diamond can retrieve primary geological information of the interior of our planet. If A and B centers are both present in diamond, their concentrations can then be used to obtain mantle storage temperatures, employing the rate of nitrogen aggregation as a thermo-chronometer and providing the mantle storage duration. The content of N (A, B center) in the sample is listed in detail in Table 2. The N content of diamond ranges from 0 to 540 ppm, the temperature from 1092 to 1173 °C and the distribution diagram of nitrogen content is shown in Figure 4a. The comparison of the N content of kimberlite diamonds in different areas is shown by the box diagram in Figure 4b and it can be concluded that their N content is not very different.

Table 2. N contents and formation temperature of diamonds in three belts calculated by software QUIDDIT. [NA], [NB], [Nt] mean concentration of nitrogen in A, B center and total nitrogen content, respectively.

Belt	Sample Name	[NA]/ppm	[NB]/ppm	[Nt]/ppm	T/°C
Changmazhuang	SLI-7	141	0	141	nan
	SLI-2	139	0	139	nan
	SLI-4	15	0	15	nan
	SLI-3	11	0	11	nan
	HQ27-1-3.	8	0	8	nan
	HQ27-1-2	0.2	0	0.2	nan
Xiyu	HQ23-6	168	371	539	1147
	HQ23-03	408	79	487	1092
	HQ23-02	82	247	329	1167
	HQ23-9	205	0	205	nan
	HQ23-05	134	0	134	nan
	HQ23-12-2	76	0	76	nan
	HQ23-11-2	70	0	70	nan
	HQ23-14.1	54	0	54	nan
Poli	29Z4	2	0	2	nan
	35T-02	183	131	314	1133
	Q29-5	243	0	243	nan
	PO-1	84	0	84	nan
	Q29-7	32	17	49	1173
	Q29-1	29	0	29	nan
	Q29-3	23	0	23	nan
	Q29-4	17	0	17	nan
	PO-2	0	0	0	nan
Q29-1	0	0	0	nan	

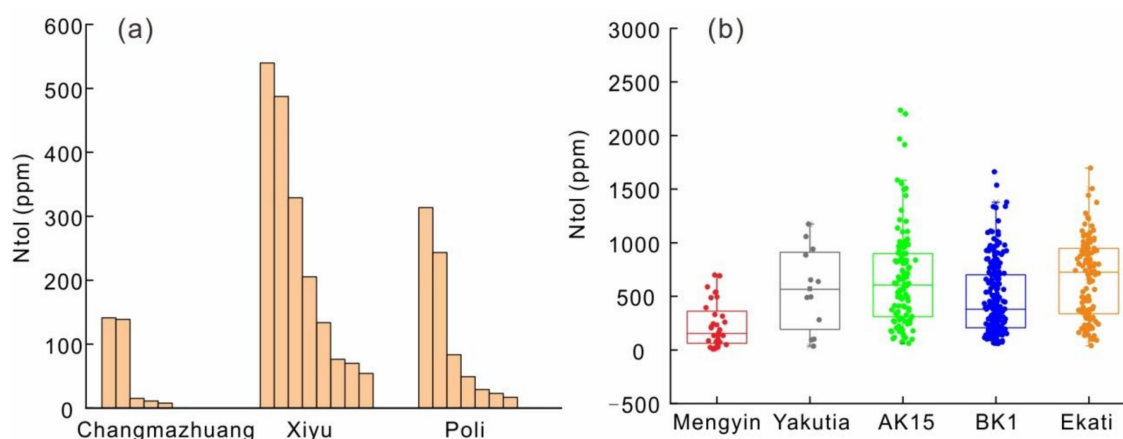


Figure 4. (a) Distribution diagram of N content in studied diamonds from the Poli, Xiyu and Chuangmazhuang belts; (b) Plot of N content of diamonds from different deposits worldwide: Mengyin deposit from Shandong province, China; Yakutia deposit from Russia; AK15 and BK1 mines from Orapa cluster, Botswana; Ekati deposit from Northwest Territories, Canada [19,20].

4.3. Raman Spectral Features

Raman spectroscopy is used to study the microstructure of molecules or substances of crystals and widely employed to characterize the lattice dynamics of diamond [12,21]. The full width at half maximum (FWHM) of the laser Raman spectrum peak is an important manifestation of diamond crystallinity and is related to the degree of internal strain and defects in diamond crystal. The value of FWHM is inversely proportional to the crystallinity of diamond [22].

The FWHM data for all studied samples ranges from 5 to 7 cm^{-1} , with an average value of 6 cm^{-1} (Table 3). The FWHM values of diamonds from Changmazhuang, Xiyu and Poli belts are 5–7 cm^{-1} (average 6 cm^{-1}), 5–8 cm^{-1} (average 6 cm^{-1}) and 5–7 cm^{-1} (average 6 cm^{-1}), respectively, indicating that the crystallization degree of diamond in the three belts is consistent. The strong intrinsic peak due to diamond's sp^3C structure in the Raman spectra of all studied diamonds shows no difference in degree of drift to low wavenumber, compared to a diamond with a perfect lattice with a characteristic Raman peak of 1332 cm^{-1} (Figure 5). The characteristic peaks of studied diamonds range from 1330 to 1331 cm^{-1} , with an average value of 1331 cm^{-1} in the Changmazhuang belt, range from 1330 to 1332 cm^{-1} , with an average value of 1331 cm^{-1} in the Xiyu belt, and show an average value of 1331 cm^{-1} in the Poli belt (Table 3).

Table 3. Raman spectra of studied diamonds in the three belts.

Belt	Sample	Center (cm^{-1})	Width (cm^{-1})	Height (Count)	
Changmazhuang	SL-1	1331	6	138,191	
	SL-2	1331	6	120,251	
	SL-3	1331	6	146,168	
	SL-4	1331	5	105,104	
	SL-5	1331	6	133,836	
	SL-6	1331	6	106,812	
	SL-7	1331	6	95,520	
	SL-8	1331	6	130,650	
	HQ27-1	1331	7	117,297	
	HQ27-2	1330	6	63,842	
	HQ27-3	1331	6	58,417	
	HQ27-4	1331	6	130,451	
	HQ27-5	1331	6	141,203	
	HQ27-6	1331	5	97,858	
	Xiyu	HQ23-1	1331	7	102,759
		HQ23-2	1331	6	21488
HQ23-3		1331	6	147,178	
HQ23-4		1331	6	114,116	
HQ23-5		1332	8	55,387	
HQ23-6		1331	6	131,072	
HQ23-7		1331	6	109,617	
HQ23-8		1331	6	146,064	
HQ23-9		1331	5	138,451	
HQ23-10		1331	6	127,246	
HQ23-11		1331	6	143,286	
HQ23-12		1331	6	122,725	
HQ23-14		1330	6	143,345	
HQ23-15		1331	6	127,433	
HQ23-16		1331	7	97,199	
Poli		Q29-1	1331	6	121,981
	Q29-2	1331	5	133,721	
	Q29-3	1331	6	106818	
	Q29-4	1331	6	137289	
	Q29-5	1331	6	137074	
	Q29-6	1331	6	23953	
	Q29-7	1331	5	131261	
	35T10-1	1331	6	148989	
	35T10-2	1331	7	110251	
	35T10-3	1331	6	137446	
	PO-1	1331	6	132318	
PO-2	1331	6	25710		
29Z4	1331	6	23086		
Average		1331	6	111496	

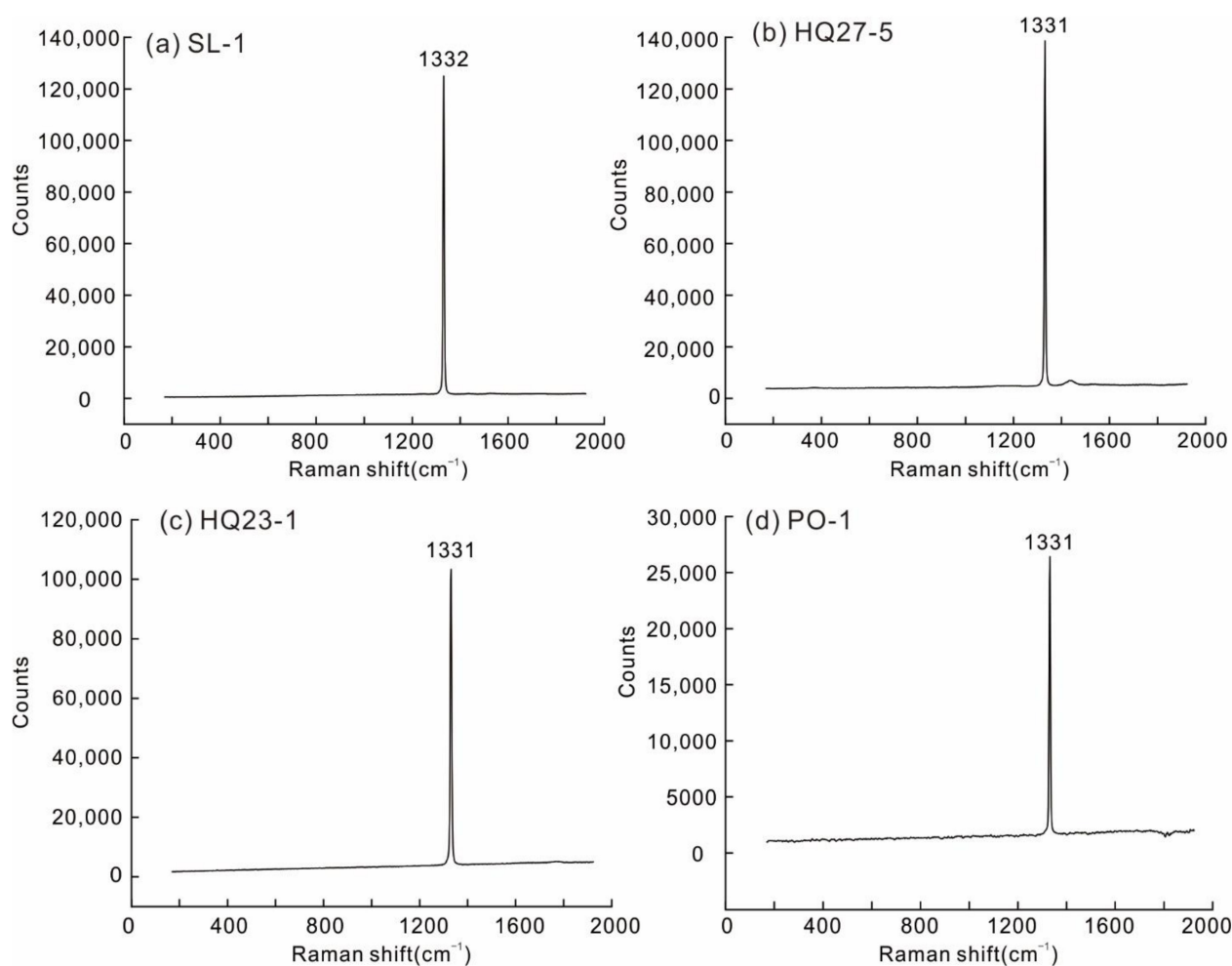


Figure 5. Raman spectra of representative diamond samples in three kimberlite belts. (a) Sample SL-1 and (b) sample HQ27-5 in the Changmazhuang belt; (c) Sample HQ23-1 in the Xiyu belt; (d) Sample PO-1 in the Poli belt.

5. Discussion

5.1. Diamond Formation Temperature

The formation temperature of diamond can be acquired from their inclusions and FTIR spectra [18]. The temperature of brown diamonds in Shengli I pipe ranges from 1118 °C to 1251 °C [12], which overlaps with those with equilibrium temperature of 1184 °C, based on diamond inclusions in Mengyin deposit [23]. Previous studies in general focused on diamonds from Shengli I pipe in the Changmazhuang belt, while the data for Xiyu diamonds is rare and there is no data for Poli diamonds.

The temperature range of diamond formation in the three belts is obtained from the conversion rate of A and B centers of diamond (Figure 3). Our results show that the temperature range of crystal formation is 1091–1167 °C for Xiyu diamonds and 1132–1172 °C for Poli diamonds. The temperature range of diamond formation is consistent with the values of 1083–1194 °C in North China craton [20]. We do not have the temperature values for Changmazhuang diamonds, because all the studied diamonds in the Changmazhuang belt are dominant type IaA with minor type II. Compiled with previous studies [12,23,24], we put forward a range of 1118–1251 °C for the Changmazhuang diamonds. The data is obviously higher than those for diamonds in Xiyu and Poli belts in this study.

5.2. The Surface Texture of Diamond: Residence in Mantle

Surface resorption of diamond is mainly composed of pre-kimberlitic and kimberlitic surface features [20], related to diamond growth and residence in the mantle, and to the process of diamonds carried to the surface of our planet by kimberlite or lamproite magmatism [5,12,25]. During mantle residence, diamonds experience partial resorption due to mantle metasomatism and, during ascent in kimberlite magma, diamonds react with evolving kimberlite which can fully or partially cover surface features caused during mantle residence. However, some diamonds are enclosed inside mantle xenoliths during the whole duration of ascent in kimberlite magma, which can preserve their pre-kimberlite surface features and records that the last diamond-destructive metasomatic event occurred in the deep mantle [20,26].

Rounding glossy crystal edges and ditrigonal shape of {111} faces leading to THH crystal morphology are common features of all the various styles of kimberlitic resorption, whereas sharp-edged octahedral diamonds and the undamaged (complete) trigonal shape of {111} faces indicate that they were likely not to have been exposed in kimberlite magma [6,27]. Meanwhile, thick step-faces with triangular shape and sharp edges form during growth. Thick steps with irregular outline and/or rounded edges and thin triangular or serrate laminae are considered to be the result of resorption [28]. Fedortchouk et al. studied diamonds from Ekati mine in Northwest Territories, Canada, Snap Lake kimberlite dyke, Northwest Territories, Canada, and Orapa cluster in Botswana and proposed four main types of pre-kimberlite resorption features including (1) Deep Pits+/-Knobs, Plates, (2) Octa with features on {111} faces, (3) Ribbed dodecahedra, (4) Laminae (Serrate/Triangular). Ribbed dodecahedra are relatively rare and present only in some diamonds. Different types of step-faces and laminae have been found in many octahedral diamonds [20]. The intensity and geometry of the surface features in diamond depend on the resorption conditions, and the most important factor controlling resorption features of diamonds at mantle conditions is the state of the diamond-dissolving metasomatic agent of fluid or melt [26]. It is proven that what is destructive to diamond is carbonate-silicate melt-driven metasomatism in the mantle, not metasomatism by C–O–H fluid [5].

In Mengyin deposit, diamonds in the three belts have complex pre-kimberlite surface features. The obviously sharp triangular growth plate with pre-kimberlite morphology is observed in all three belts (Figure 6). They all have uniform pre-kimberlite surface features of multiple serrate, triangular laminae and small trigons (Figure 2a,b,i,k), of which the triangular laminae and multiple serrate on Changzhuang and Xiyu diamonds (Figure 6a–d) and on Poli diamonds (Figure 2k,i) were reproduced in experiment with metasomatism caused by carbonatitic and silicate-carbonatitic melts [5]. Similar pre-kimberlite resorption styles on diamonds in three belts are likely to show uniform conditions of diamond destructive metasomatism. However, octahedra diamonds with step-faces of multiple terraces are commonly observed on Changmazhuang and Xiyu diamonds (Figure 6a–d), suggesting that they may develop in a hydrous carbonatitic melt at $T < 1450$ °C [5]. Meanwhile, rare surface features of ribbed dodecahedra and uncommon terraces are observed in Poli diamonds (Figure 6e,f), their diamond terraces are exhibited as more regular and sharper (Figures 2k and 6f) and they develop shallow flat-bottomed trigons on surfaces (Figure 2i), implying that the Poli diamonds were probably metasomatized by a silicate component-enriched carbonatitic melt in deep the mantle, compared with their two counterparts.

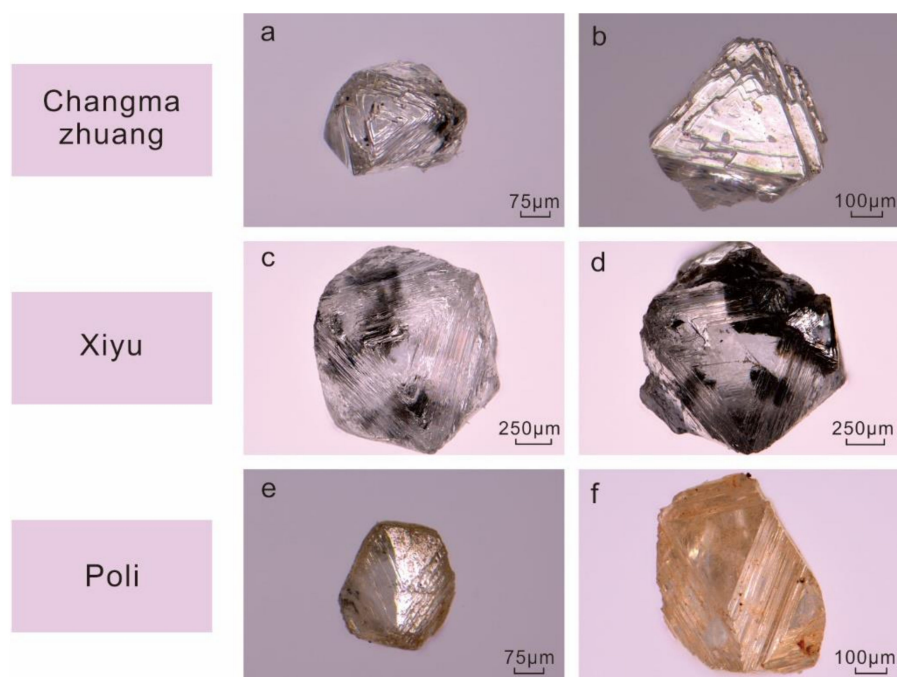


Figure 6. Pre-kimberlite surface textures of diamonds from three belts in Mengyin deposit. (a) Samples SL1-2 and (b) SL-7 from the Changmazhaung belt showing serrate laminae; (c) samples HQ23-13 and (d) HQ23-15 from the Xiyu belt showing triangular laminae; (e) samples Q29-3 and (f) Q29-7 from the Poli belt showing ribbed dodecahedra.

5.3. Relationship between N Impurity and Surface Texture

Diamond with a perfect lattice is generally transparent and colorless, but it is rare to find diamonds without impurities and defects. Significant information about the growth history of diamond can be revealed by FTIR spectra, which define the spatial distribution of impurities in the diamond. Most natural diamond (>90%) contains nitrogen, which is the most important impurity which affects color, diversity and thermal conductivity [29]. Type classification of diamond depends on the absence of nitrogen and boron atom and their aggregation states in the diamond lattice (Figure 7).

The aggregation sequence of the nitrogen in diamond gradually changes over time. At first, nitrogen appears in diamond as a single atom (C center, FTIR at 1130 cm^{-1}). Two neighboring monatomic nitrogen atoms will be combined into one nitrogen pair (A center, FTIR at 1282 cm^{-1}). Then, under the action of high temperature, the nitrogen pairs will migrate and form four nitrogen atoms surrounding one vacancy (B center, FTIR at 1175 cm^{-1}). The B center can further aggregate to form submicroscopic inclusion nitrogen crystals (inclusions can be recognized by electron microscope), which are called platelets, because they are usually distributed along a specific surface network (such as $\{111\}$ plane) and are in two-dimensional extension (B', FTIR at $1365\text{--}1375\text{ cm}^{-1}$). Hydrogen is the second most abundant impurity in natural diamonds after nitrogen, which can also be associated with nitrogen atoms or vacancies [30].

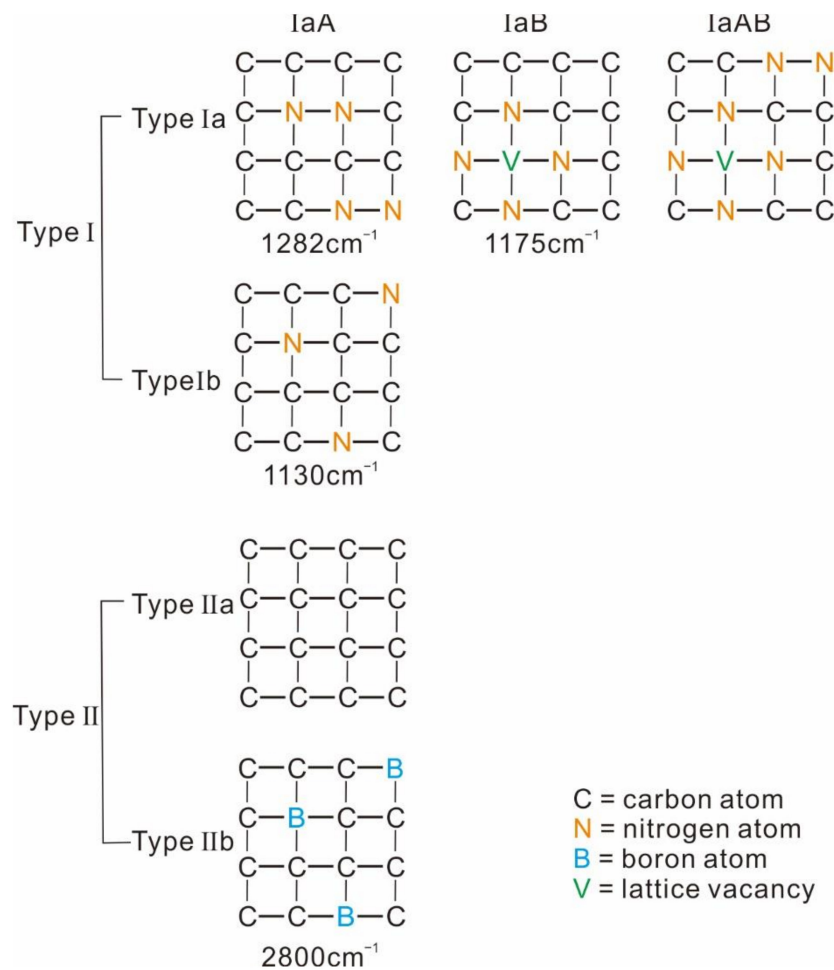


Figure 7. N and B atoms replace C atoms in various types of diamond lattice [31].

There is controversy as to whether the impurity N has an influence on diamond resorption. Fedortchouk et al. carried out dissolution experiments of diamonds with different N contents at the condition of the mantle. Diamond samples cover a range of nitrogen content from 35 to 1173 ppm, and aggregation from 10 to 76% of B-defects, while the results for diamonds with different nitrogen concentration produced very similar resorption features. This experimental result indicates no effect of nitrogen defects in diamonds on their resorption. The experiments with the condition of kimberlite magma (1150–1500 °C, 1 Gpa) also indicates no correlation between the rate and character of diamond oxidation and physical properties of diamonds (nitrogen content, color) [26]. Yang et al. studied the relationship between surface morphology and N content of diamonds from Yuanshui Hunan province; the nitrogen content was 22.90–752.4 $\mu\text{g}\cdot\text{g}^{-1}$ /ppm and the aggregation of B-defects 22.35–55.58%. It was found that the low nitrogen content is beneficial to the formation of triangular growth lamellae and other morphologies, while the high nitrogen content is more beneficial to the formation of spiral growth line and other morphologies. In this study, diamond samples cover a range of nitrogen content from 0–539.53 ppm. Resorption of studied diamonds has no obvious relationship with nitrogen concentration.

6. Conclusions

The formation temperature is 1091–1167 °C for Xiyu diamonds, and 1132–1172 °C for Poli diamonds, their values slightly lower than those of 1118–1251 °C for the Changmazhuang diamonds [12].

The nitrogen contents of 44 studied diamonds in the three belts are different, but having no obvious relationship with resorption on diamonds. The crystallization degree of

diamonds in the three belts is consistent based on average FWHM value of diamonds from the Poli, Xiyu and Changmazhuang belts.

Diamonds in the three belts exhibit uniform pre-kimberlite surface features of multiple serrate, triangular laminae and small trigons, suggesting a similar condition of diamond destructive metasomatism caused by carbonatitic and silicate-carbonatitic melts during residence in the mantle. However, Poli diamonds were probably metasomatized by a silicate component-enriched carbonatitic melt in the deep mantle, compared with its two counterparts.

Author Contributions: Conceptualization, C.-F.Z., F.L. and J.-S.Y.; methodology, C.-F.Z., F.L., Q.L. and Y.W.; software, C.-F.Z. and F.L.; validation, C.-F.Z., F.L. and J.-S.Y.; formal analysis, C.-F.Z., F.L. and Q.L.; investigation, F.L. and J.-S.Y.; resources, F.L., Q.L. and J.-S.Y.; data curation, C.-F.Z., F.L. and Q.L.; writing—original draft preparation, C.-F.Z. and F.L.; writing—review and editing, C.-F.Z. and F.L.; visualization, C.-F.Z. and F.L.; supervision, F.L.; project administration, F.L., J.-S.Y. and Q.L.; funding acquisition, F.L., J.-S.Y. and Q.L. All authors have read and agreed to the published version of the manuscript.

Funding: This research was funded by grants from the 7th Institute of Geology & Mineral Exploration of Shandong Province (QDKY202007), Shandong Provincial Natural Science Foundation (ZR2021MD052), Key Special Project for Introduced Talents Team of Southern Marine Science and Engineering Guangdong Laboratory (Guangzhou) (GML2019ZD0201), National Science Foundation of China (92062215; 41720104009), China Geological Survey (DD20221630), Key Laboratory of Deep-Earth Dynamics of the Ministry of Natural Resources (J1901-32) and State Key Laboratory of Geological Processes and Mineral Resources, China University of Geosciences (GPMR202115).

Data Availability Statement: Not applicable.

Acknowledgments: We are deeply grateful for Zhi-Yuan Chu, Bing-Jian Xiao, Dong-Yang Lian, Hui-Chao Rui, Wei-Wei Wu, Chu-Qi Chu for their help and valuable comments. We also thank two anonymous reviewers and academic editors for their valuable and constructive comments and suggestions toward improving the manuscript.

Conflicts of Interest: The authors declare no conflict of any interest in this paper.

References

1. Alvaro, M.; Angel, R.J.; Nestola, F. Inclusions in diamonds probe Earth's chemistry through deep time. *Commun. Chem.* **2022**, *5*, 10. [[CrossRef](#)]
2. Yang, J.; Wu, W.; Lian, D.; Rui, H. Peridotites, chromitites and diamonds in ophiolites. *Nat. Rev. Earth Environ.* **2021**, *2*, 198–212. [[CrossRef](#)]
3. Liu, F.; Lian, D.; Wu, W.; Yang, J. Diamonds and other exotic minerals-bearing ophiolites on the globe: A key to understand the discovery of new minerals and formation of ophiolitic podiform chromitite. *Crystals* **2021**, *11*, 1362. [[CrossRef](#)]
4. Mitchell, R.H. Potassic Alkaline Rocks: Leucitites, Lamproites, and Kimberlites. In *Encyclopedia of Geology*, 2nd ed.; Alderton, D., Elias, S.A., Eds.; Academic Press: Oxford, UK, 2021; pp. 215–239.
5. Fedortchouk, Y.; Liebske, C.; Mccammon, C. Diamond destruction and growth during mantle metasomatism: An experimental study of diamond resorption features. *Earth Planet. Sci. Lett.* **2019**, *506*, 493–506. [[CrossRef](#)]
6. Fedortchouk, Y.; Chinn, I.L.; Kopylova, M.G. Three styles of diamond resorption in a single kimberlite; effects of volcanic degassing and assimilation. *Geology* **2017**, *45*, 871–874. [[CrossRef](#)]
7. Kozai, Y.; Arima, M. Experimental study on diamond dissolution in kimberlitic and lamproitic melts at 1300–1420 °C and 1 GPa with controlled oxygen partial pressure. *Am. Mineral.* **2005**, *90*, 1759–1766. [[CrossRef](#)]
8. Gurney, J.J.; Hildebrand, P.R.; Carlson, J.A. The morphological characteristics of diamonds from the Ekati property, Northwest Territories, Canada. *Lithos* **2004**, *77*, 21–38. [[CrossRef](#)]
9. Howarth, G.H.; Sobolev, N.V. 3-D X-ray tomography of diamondiferous mantle eclogite xenoliths, Siberia: A review. *J. Asian Earth Sci.* **2015**, *101*, 39–67. [[CrossRef](#)]
10. Liu, Y.; Taylor, L.A.; Sarbadhikari, A.B.; Valley, J.W.; Ushikubo, T.; Spicuzza, M.J.; Kita, N.; Ketcham, R.A.; Carlson, W.; Shatsky, V.; et al. Metasomatic origin of diamonds in the world's largest diamondiferous eclogite. *Lithos* **2009**, *112*, 1014–1024. [[CrossRef](#)]
11. Robinson, D.N. Surface Textures and Other Features of Diamonds. Ph.D. Thesis, University of Cape Town, Cape Town, South Africa, 1979.
12. Wu, G.; Yu, X.; Liu, F.; Li, H.; Long, Z.; Wang, H. Color Genesis of Brown Diamond from the Mengyin Kimberlite. *China, Crystals* **2022**, *12*, 449. [[CrossRef](#)]

13. Ni, P.; Zhu, R. Evaluating the diamond potential of kimberlite-hosted diamond deposits from the North China Craton. *Acta Geol. Sin.* **2020**, *94*, 2557–2573.
14. Speich, L.; Kohn, S.C. QUIDDIT—QUantification of infrared active Defects in Diamond and Inferred Temperatures. *Comput. Geosci.* **2020**, *144*, 104558. [[CrossRef](#)]
15. Chu, Z. Study on Characteristics and Diamondiferous Significance of the Mengyin Kimberlite in Shandong Province. Master Degree, China University of Geosciences, Beijing, China, 2019; pp. 1–73.
16. Lv, Q.; Liu, F.; Chu, Z.; Ge, Y.; Liu, X.; Jiao, Y. The mineralogical characteristics and comparison of diamonds in the three Kimberlite belts in Mengyin, Shandong Province. *Acta Geol. Sin.* **2022**, *96*, 1225–1238.
17. Song, M.; Yu, X.; Song, Y.; Xiao, B.; Zhou, D.; Gao, C. Types, sources, and regional crust-mantle evolution background of diamonds in the western Shandong Province. *Acta Geol. Sin.* **2020**, *94*, 2606–2625.
18. Zhou, D.; Wang, W.; Yang, D. *The road of Diamond*; Geology Publishing House: Beijing, China, 2005; pp. 1–103.
19. Zhang, B.; Chen, H.; Qiu, Z. *Study on the Origin of Diamonds under the Framework of United Nations Kimberley Process*, 1st ed.; Geological Publishing House: Beijing, China, 2013; pp. 189–225.
20. Fedortchouk, Y.; Chinn, I.L.; Perritt, S.H.; Zhang, Z.; Stern, R.A.; Li, Z. Diamond-destructive mantle metasomatism: Evidence from the internal and external textures of diamonds and their nitrogen defects. *Lithos* **2022**, *414–415*, 106616. [[CrossRef](#)]
21. FerrariCarlo, A. Determination of bonding in diamond-like carbon by Raman spectroscopy. *Diam. Relat. Mater.* **2002**, *11*, 1053–1061.
22. Jian-Hong, L.; Mei-Hua, C.; Gai, W.U.; Ni-Na, G. Study on the Evaluation of the Crystal Quality of Diamonds. *J. Synth. Cryst.* **2014**, *43*, 559–564.
23. Chi, J.; Lu, F. *Characteristics of Kimberlite and Paleozoic Lithosphere Mantle in North China Platform*; Science Press: Beijing, China, 1996.
24. Yin, Z.; Lu, F.; Chen, M.; Xu, H. Ages and environments of formation of diamonds in Mengyin County, Shandong Province. *Earth Sci. Front.* **2005**, *12*, 8.
25. Yang, Z.; Mao, M.; Huang, Y.; Zhang, J. Study on the Surface Morphology and Its Vibrational Spectra of Diamond from the Western Yangtze Craton. *Spectrosc. Spectr. Anal.* **2022**, *42*, 236–242.
26. Fedortchouk, Y.; Canil, D.; Semenets, E. Mechanisms of diamond oxidation and their bearing on the fluid composition in kimberlite magmas. *Am. Mineral.* **2007**, *92*, 1200–1212. [[CrossRef](#)]
27. Zhang, Z.; Fedortchouk, Y. Records of mantle metasomatism in the morphology of diamonds from the Slave craton. *Eur. J. Mineral.* **2012**, *24*, 619–632. [[CrossRef](#)]
28. Fedortchouk, Y. A new approach to understanding diamond surface features based on a review of experimental and natural diamond studies. *Earth-Sci. Rev.* **2019**, *193*, 45–65. [[CrossRef](#)]
29. Gu, T.; Wang, W. Optical defects in milky type IaB diamonds. *Diam. Relat. Mater.* **2018**, *89*, 322–329. [[CrossRef](#)]
30. Gu, T.; Ohfuji, H.; Wang, W. Origin of milky optical features in type IaB diamonds: Dislocations, nano-inclusions, and polycrystalline diamond. *Am. Mineral.* **2019**, *104*, 652–658. [[CrossRef](#)]
31. Breeding, C.M.; Shigley, J.E. The “type” classification system of diamonds and its importance in gemology. *Gems Gemol.* **2009**, *45*, 96–111. [[CrossRef](#)]